Cerebral Cortex, 2017; 1–14

doi: 10.1093/cercor/bhx084
Original Article

ORIGINAL ARTICLE

Sensory Deprivation Triggers Synaptic and Intrinsic Plasticity in the Hippocampus

Hila Milshtein-Parush[1,2], Samuel Frere[1], Limor Regev[3], Coren Lahav[1,2], Amit Benbenishty[2,4], Shamgar Ben-Eliyahu[2,4], Inbal Goshen[3] and Inna Slutsky[1,2]

[1]Department of Physiology and Pharmacology, Sackler Faculty of Medicine, Tel Aviv University, Tel Aviv 69978, Israel, [2]Sagol School of Neuroscience, Tel Aviv University, Tel Aviv 69978, Israel, [3]The Edmond and Lily Safra Center for Brain Sciences, The Hebrew University, Jerusalem 91904, Israel and [4]Neuroimmunology Research Unit, School of Psychological Sciences, Tel Aviv University, Tel Aviv 69978, Israel

Address correspondence to Inna Slutsky. Email: islutsky@post.tau.ac.il

H. Milshtein-Parush and S. Frere contributed equally to this work

Abstract

Hippocampus, a temporal lobe structure involved in learning and memory, receives information from all sensory modalities. Despite extensive research on the role of sensory experience in cortical map plasticity, little is known about whether and how sensory experience regulates functioning of the hippocampal circuits. Here, we show that 9 ± 2 days of whisker deprivation during early mouse development depresses activity of CA3 pyramidal neurons by several principal mechanisms: decrease in release probability, increase in the fraction of silent synapses, and reduction in intrinsic excitability. As a result of deprivation-induced presynaptic inhibition, CA3-CA1 synaptic facilitation was augmented at high frequencies, shifting filtering properties of synapses. The changes in the AMPA-mediated synaptic transmission were accompanied by an increase in NR2B-containing NMDA receptors and a reduction in the AMPA/NMDA ratio. The observed reconfiguration of the CA3-CA1 connections may represent a homeostatic adaptation to augmentation in synaptic activity during the initial deprivation phase. In adult mice, tactile disuse diminished intrinsic excitability without altering synaptic facilitation. We suggest that sensory experience regulates computations performed by the hippocampus by tuning its synaptic and intrinsic characteristics.

Key words: hippocampus, intrinsic excitability, sensory deprivation, synaptic plasticity, whisker trimming

Introduction

A fundamental feature of neural circuits is the capacity for plasticity in response to experience. Synaptic plasticity is known to be essential for achieving the proper organization of neural circuits during early development, as well as for the processing, storage, and retrieval of information in matured neural circuits. Pioneering studies by Hubel and Wiesel (Wiesel and Hubel 1963) demonstrated the existence of a critical period in early postnatal development during which depriving an eye of visual input dramatically alters thalamocortical projections in favor of the open eye. Since then, refinement of synaptic connections has been widely documented by

visual, somatosensory or auditory deprivation in the corresponding primary sensory cortex (Hensch 2005; Feldman 2009; Smith et al. 2009). However, very little is known about how sensory experience shapes neural circuits in structures higher in the hierarchy of information processing that receive multimodal sensory inputs.

The hippocampus, a temporal lobe structure critical for learning and memory of events and space (Squire et al. 2004), constitutes one of the convergent zones of cortical processing and receives inputs from all the sensory modalities (Lavenex and Amaral 2000). The entorhinal cortex serves as an anatomical gateway through which the majority of cortically processed information is presented to the hippocampus. This cortical information is relayed directly via monosynaptic connections to the CA3, CA1, and dentate gyrus hippocampal subregions (Witter et al. 1989) or indirectly via the serial connections of the trisynaptic circuit. In accordance with this organization, hippocampal lesions impair memory irrespective of the sensory modality in which information is presented (Squire et al. 2004).

The hippocampus has long been a key experimental system for studying activity-dependent synaptic plasticity. Unlike the synapses in primary sensory cortices, hippocampal connections maintain substantial capacity for activity-dependent plasticity throughout adulthood. However, how the history of sensory experience regulates the functioning of hippocampal neurons remains obscure. Our early study suggests that visual deprivation during the critical period of visual cortex plasticity regulates synaptic facilitation in the rat hippocampus (Dolev et al. 2013). This intriguing finding triggered us to explore systematically how sensory stimuli, playing a critical role during early postnatal development, regulate synaptic and intrinsic properties of hippocampal neurons. Our study revealed a remarkable functional plasticity in the CA3 and CA1 hippocampal regions of mice by whisker deprivation, emphasizing a critical role for tactile experience in shaping neuronal computations performed by the hippocampus.

Materials and Methods

Animals

All animal experiments were approved by the Tel Aviv University Committee on Animal Care. All animals were kept in a normal light/dark cycle (12 h/12 h). Animals were raised with their mother until the end the weaning period (end of third week). Bilateral whisker trimming was performed daily from postnatal day 10 (P10), or from P28, by cutting the mystacial vibrissae to skin level with fine scissors, under isoflurane anesthesia. Control mice were housed together with deprived mice and handled under identical isoflurane conditions for the same duration. No change in body weight and motor function (see Supplementary Fig. 8) of mice were observed during the deprivation period.

Slice Preparation and Electrophysiology

On the day of recording the brains were quickly removed and transverse slices (400 μm for field recordings, 350 μm for whole-cell recordings) of hippocampus were prepared in an ice-cold storage buffer containing (in mM): sucrose, 206; KCl, 2; $MgSO_4$, 2; NaH_2PO_4, 1.25; $NaHCO_3$, 26; $CaCl_2$, 1; $MgCl_2$, 1; glucose, 10. The slicing procedure was performed using a Leica VT1200 vibrating microtome. Slices were then transferred to a submerged recovery chamber at room temperature containing oxygenated (95% O_2 and 5% CO_2) artificial cerebrospinal fluid (ACSF) for 1 h before the measurements. The ACSF contained, in mM: NaCl, 125; KCl, 2.5; $CaCl_2$, 1.2; $MgCl_2$, 1.2; $NaHCO_3$, 25; NaH_2PO_4, 1.25; glucose, 25.

All recordings were performed at room temperature, except Supplementary Figure 1A–C, in a recording chamber on the stage of an Olympus BX51WI microscope equipped with IR DIC optics. Stimulation of the Schaffer Collateral (SC) was delivered through a glass suction electrode (10–20 μm tip) filled with ACSF. fEPSPs were recorded using a glass pipette containing ACSF (1–2 MΩ) from proximal synapses in the CA1 stratum radiatum. Whole-cell patch pipettes (2–3 MΩ) were used to record EPSCs from CA1 neurons using the following intracellular solution (in mM): Cs-$MeSO_3$, 102; HEPES, 10; CsCl, 3.5; Na_2Phosphocreatine, 5; CaCl2, 1; Na-ATP, 2; Na_3GTP, 0.3; EGTA, 0.5; MgCl2, 0.5; Cs_4BAPTA, 10; pH adjusted to 7.25 with NaOH. For short-term potentiation recordings, 2 mM QX314-chloride was added to the intracellular solution and amino-phosphonopentanoate (AP-5; 100 μM) was added to the extracellular solution. For NMDAR currents recordings, ACSF contained 20 μM DNQX, and 10 μM bicuculline. For mEPSCs and AMPA IV curve recordings the following intracellular solution was used (in mM): Cs-$MeSO_3$, 120; HEPES, 10; NaCl, 10; $CaCl_2$, 0.5; Mg^{2+}-ATP, 2; Na_3GTP, 0.3; EGTA, 10; pH adjusted to 7.25 with NaOH. For AMPA IV curve, 0.1 mM spermine was also added to the intracellular solution, while AP-5 (100 μM), and bicuculline (10 μM) were added to the extracellular solution. For mEPSCs recordings, ACSF contained tetrodotoxin (TTX; 1 μM), 100 μM AP-5, 10 μM bicuculline and $CaCl_2$ concentration was raised to 2.5 mM in order to increase the frequency of events.

For minimal stimulation (Figs 2A,B and 5D), used to putatively stimulate one axonal fiber making synaptic contacts on the CA1 cell recorded from, the following criteria were used (Dobrunz and Stevens 1997; Hanse and Gustafsson 2001): 1) the constancy of response amplitude during a 50 Hz burst stimulation following 2 consecutives increment of 10% of the stimulation intensity; 2) the quantitative characteristics of the synaptic response remain invariant throughout experiment; and 3) reducing stimulation intensity leads abruptly to a complete failure of responses. We recorded 200–250 consecutive sweeps for each cell in presence of 50 μM APV. Stimulation was evoked at 0.5 Hz at the holding potential of −70 mV. Failures versus successes were defined visually. Coefficient of variation (CV) was calculated as: $(SD_{EPSC}{}^2)$/Mean EPSC amplitude.

For silent synapses (Fig. 4A,B), ACSF contained 10 μM SR-95531 (gabazine) and $CaCl_2$ and $MgCl_2$ concentrations were modified in the ACSF solution to 4 mM.

For pressure application of glutamate (Fig. 5E,F), ACSF contained 1 μM TTX and 100 μM AP-5 and the intracellular solution contained (in mM): K-Gluconate, 112; KCl, 8 mM; HEPES, 10; $MgCl_2$, 0.5; $CaCl_2$, 0.5; EGTA, 5; Na-phosphocreatine, 10; Na_2-ATP, 4; GTP, 0.4 and AlexaFluor488, 0.06 to visualize the dendritic spines after recording. Current induced by glutamate was recorded while the membrane potential was held at −65 mV. A glass electrode (7–8 MΩ) filled with 5 mM glutamate dissolved in ACSF was connected to a Picospritzer III (Parker Hannifin Corporation, Fairfield, NJ), which delivered brief air puffs (from 3 to 6.5 ms at 5 p.s.i., in a 0.5 ms increment). The puff pipette was lowered into the slice and placed at 100–150 μm distance from the pyramidal layer. The localization of the pipette was optimized to get the maximal current amplitudes.

For intrinsic excitability measurements (Figs 6 and 7F,G), the following intracellular solution was used (in mM): Kgluconate, 120; KCl, 10; HEPES, 10; Na_2Phosphocreatine, 10, Na_2ATP, 4; Na_3GTP, 0.3; $MgCl_2$, 0.5; pH adjusted to 7.25 with NaOH. Frequency versus current intensity curves were plotted by measuring the average rate of action potentials in current clamp during 500-ms long depolarizing steps of increasing intensity in the presence of synaptic blockers (100 μM AP-5, 20 μM DNQX, and

10 μM bicuculline). If the resting potential of a neuron differed from RMP (–70 mV), a DC current was injected to bring the membrane potential to RMP. Spike threshold was measured as the interpolated membrane potential at which dV/dt equaled 20 V/s.

For all the whole-cell patch clamp recordings, serial resistance was not compensated. Neurons were excluded from the analysis if RMP was >–55 mV, serial resistance was >20 MΩ (10 MΩ for mEPSC recordings), and R_{in} was <80 MΩ or if any of these parameters changed by >20% during the recording. Signals were recorded using a MultiClamp 700B amplifier, digitized by DigiData1440A (Molecular Devices) at 10 kHz, and filtered at 2 kHz. Data were analyzed using MiniAnalysis (Synaptosoft) for mEPSCs, and pClamp10 (Molecular Devices) for evoked EPSCs and excitability measurements. For quantification of AMPA/NMDA ratio (Fig. 4*C*,*D*), the time of the peak current at –60 mV, considered to be mainly mediated by AMPAR, was used to establish the time window for measuring the AMPA peak at +40 mV. The decay to baseline of the AMPA current at –60 mV was used to select a time window for measurement of the NMDA current; a 5-ms measurement window beginning 50 ms after the stimulus artifact was used. This current was designated as the NMDA measurement. AMPA/NMDA ratio was calculated as ($I_{AMPA\ at\ +40mV}/I_{NMDA\ at\ +40mV}$).

Imaging and Image Analysis

Immediately after the end of the whole-cell recording, the patch pipette was delicately removed and the AlexaFluor488-filled pyramidal cells were imaged. Images were collected with a 20× (1.0 NA) or 63× (0.9 NA) water immersion objective (Zeiss) using a Zeiss LSM710 laser-scanning microscope controlled by the Zen 2010 software. Chameleon Ti:Sapphire laser system with a 80 MHz repetition rate (Coherent Radiation, Palo Alto, CA) was used to excite the sample at 760 nm excitation wavelength. Emitted fluorescence was detected by Zeiss BIG-2 ch GaAsP detector after being filtered with a 500–550 nm band pass filter (Chroma). The size of images of dendritic protrusions was 512 × 512 pixels at a nominal spatial resolution of 10–20 pixels per micrometer, acquired with 10–40 μm deep Z-stacks (usually composed of 20–100 images separated by 0.3–0.5 μm). Images were analyzed using the freeware NeuronStudio (developed by the Computational Neurobiology and Imaging Center of the Mount Sinai School of Medicine, New York). After automatic drawing of the dendrites, spines were semi-automatically detected: all visible spines (defined as small protrusions, at right angle to the parent dendrite, measuring up to 3–4 μm in length) were counted on clearly focused dendrites for the primary dendrites in the first 100–150 μm from soma. The spine density was calculated as the number of spines divided by the dendritic length.

Assessment of Plasma Corticosterone (CORT) Levels

Blood was withdrawn by cardiac puncture at 8 PM. To this end, animals were euthanized with isoflurane, and 50–100 μL from P11, P15, and P21 mice and 250–300 μL of blood from P50 animals was withdrawn from the heart, within less than 3 min of approaching the animals, using EDTA-containing syringes (1.8 mg/1 mL blood). Blood was then centrifuged for 20 min at 930 × *g*, 4 °C, for plasma separation, which was collected and stored at –20 °C until assayed for CORT levels. Plasma CORT levels were measured by radioimmunoassay (RIA) (ImmuChem double antibody corticosterone 125I RIA kit, MP Biomedicals, Orangeburg, NY), per manufacturer's instructions. The intra assay coefficient of variability was less than 5%, as reported by the manufacturer.

Behavioral Tests

Before each test, mice were acclimatized to the experimental room for at least 40 min. The equipment was cleaned with virusolve after each trial to remove residual odors. Behavioral data were recorded from C57BL/6 J mice by video camera (GigE color 1/2″ Basler acA1300–60gc) and analyzed using EthoVision 11.5 XT (Noldus, The Netherlands).

Open Field

Activity monitoring was conducted in a square-shaped, white Perspex open field, measuring 50 × 50 cm^2, and illuminated from above by 250 lux. Mice were placed individually into the arena for 5 min. Parameters assessed for the present study were total distance traveled and percentage of time in and number of entries to center, which was defined as the area ~12 cm distant from the walls.

Elevated Plus-Maze

The plus-maze was made from white Perspex and consisted of 2 open arms 35 × 5 cm and 2 enclosed arms 35 × 5 × 15 cm. The arms extended from a central platform of 5 × 5 cm. The plus-maze was elevated to a height of 40 cm above the floor, and illuminated from above by 250 lux. Animals were placed in one of the protected sectors and were observed for 5 min. The parameters that were analyzed are the number of entries to and the percent of time spent in the open compartments.

Chemical Reagents

TTX was purchased from Alamone Labs, DNQX, ifenprodil, spermine, bicuculline, QX-314 bromide and AP-5 from Tocris, (+)MK801 and SR-95531 from Abcam, Alexa fluor-488 from Molecular Probes.

Statistical Analysis

Error bars shown in the figures represent standard error of the mean (s.e.m.). The number of patched neurons is defined by *n*, the number of mice by *N*. Student's unpaired *t*-tests were used to compare 2 populations of neurons/mice. Student's paired *t*-tests were used in the experiments where the effect of ifenprodil was tested in the same cell ($^{*}P < 0.05$; $^{**}P < 0.01$; $^{***}P < 0.001$). Two-way ANOVA analysis, corrected for repeated measurements, was used to test the effects of deprivation and the stimulus number during spike bursts, current steps or puff duration ($^{*}P < 0.05$; $^{**}P < 0.01$; $^{***}P < 0.001$). For comparison of mEPSC amplitude or frequency under different conditions, 150 mEPSCs were randomly selected for each cell and pooled for each condition. A Kolmogorov–Smirnov (K–S) test was used to compute differences in distributions across the pooled data sets.

Results

Effect of Whisker Deprivation on CA3-CA1 Synaptic Transmission

In rodents, the highly sensitive facial whiskers are responsible for providing accurate tactile information about ongoing environmental changes. As somatosensory stimuli are likely to be predominant sensory inputs in mice during early postnatal development, we decided to focus on the effects of whisker deprivation on functioning of hippocampal synapses. Bilateral whisker trimming was performed daily in BALB/c mice from

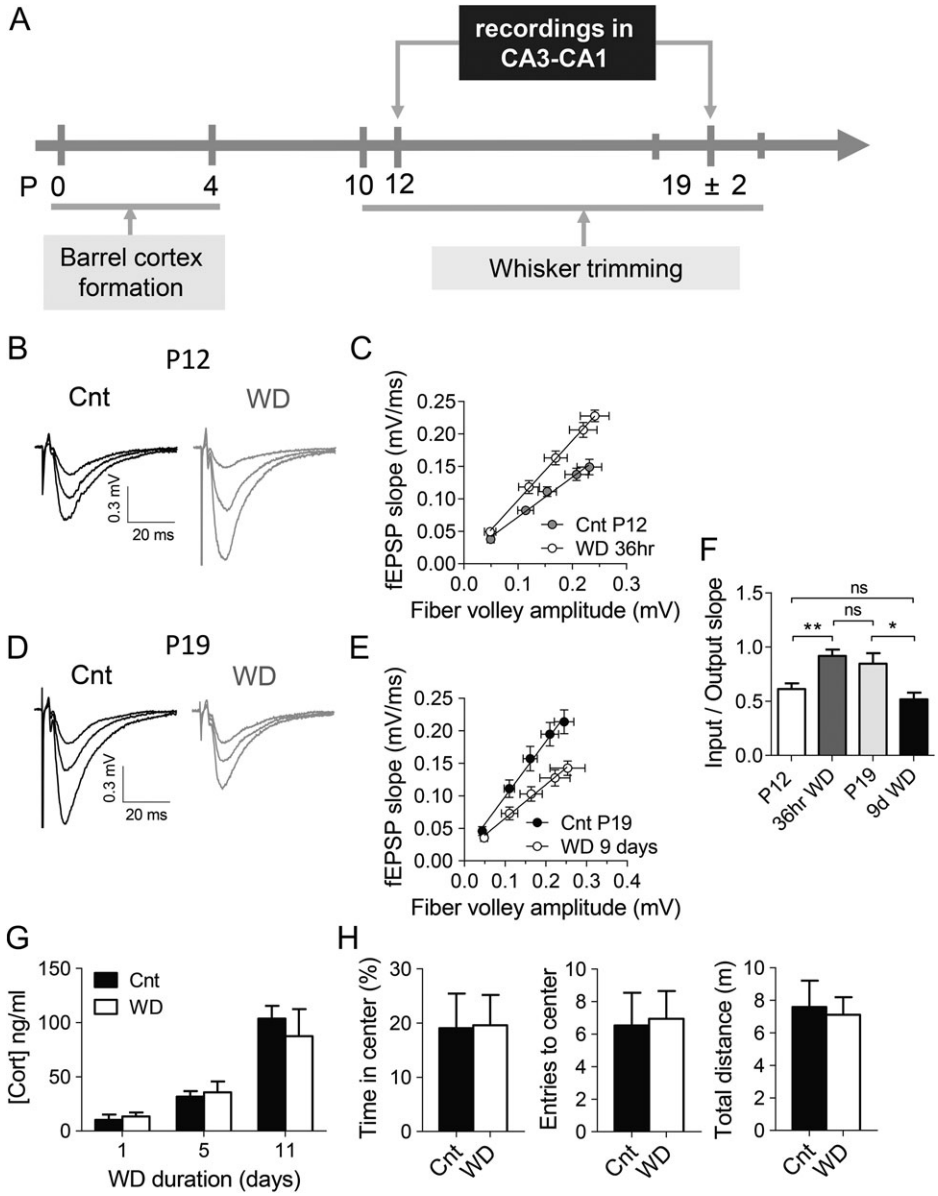

Figure 1. Long-term whisker deprivation decreases synaptic strength in the CA3-CA1 synapses without altering stress-related characteristics. (*A*) Experimental design. Whiskers were bilaterally trimmed starting at P10. Control (Cnt) group was handled under the same housing and experimental conditions. The electrophysiological data were collected at P12 (36 h after the deprivation) and at P19 ± 2. (*B*,*D*) Representative fEPSP recordings in different stimulation intensities (30, 50, and 100 μA; black—Cnt, grey—whisker deprived (WD)) at P12 (*B*) and P19 (*D*). (*C*,*E*) Input/output relationship between the amplitude of fiber volley and the slope of fEPSP for gradually increasing stimulation intensities in CA3-CA1 connections in P12 (*C*, Cnt $n = 9$, $N = 5$; WD $n = 8$, $N = 4$; $P < 0.01$) and P19 (*E*, $n = 10$, $N = 6$; $P < 0.05$) Cnt and WD mice. (*F*) Comparison of average input/output slopes for mice deprived for short-term (36 h) and long-term (9 ± 2 days) periods versus age-matched controls (the same data as in C,E). (*G*) No differences in plasma corticosterone levels were evident between Cnt and WD mice for different periods of deprivation: 1 day (WD $N = 4$, Cnt $N = 2$; $P = 0.63$), 5 days (WD $N = 4$, Cnt $N = 3$; $P = 0.77$) and 11 days (WD $N = 4$, Cnt $N = 3$; $P = 0.63$). (*H*) In the open field test, no difference was observed between WD ($N = 18$) and Cnt ($N = 17$) mice in the percent of time spent in center (left, $P = 0.95$), number of entries to center (middle, $P = 0.87$), and total distance traveled (right, $P = 0.8$). $^{*}P < 0.05$, $^{**}P < 0.01$. Unpaired 2-tailed student *t*-test. Error bars represent s.e.m.

postnatal day 10 (P10) for 36 h versus 9 ± 2 days until the day of recording (P12 vs. P19 ± 2, respectively, Fig. 1A). Control mice were housed and handled under identical conditions for the same duration. To maintain the structural anatomy of barrels during the first week (Fox 2002), we started the deprivation at the second postnatal week, corresponding to the period of extensive developmental changes in the properties of hippocampal synapses (Cull-Candy et al. 2001; Dumas 2005) and to the critical period of the layer 2/3 neurons in the barrel cortex (Stern et al. 2001).

First, we measured the effect of deprivation on input/output relationship in the CA3-CA1 synaptic connections. For this, we recorded field excitatory postsynaptic potential (fEPSP) evoked by low frequency stimulation (0.1 Hz) of CA3 axons as a function of stimulation intensity (Fig. 1B–F). The slope of input (amplitude of fiber volley)/output (slope of fEPSP) curve was increased by ~50% in the first 36 h following deprivation from 0.61 ± 0.05 to 0.92 ± 0.06 in P12 mice ($P < 0.01$, Fig. 1B,C). Notably, the input/output slope after 36 h of deprivation was similar to those of older, P19 control mice ($P = 0.92$, Fig. 1E,F).

However, longer deprivation period of 9 ± 2 days triggered a ~40% decrease in the input/output slope, resulting in 0.52 ± 0.1 slope in whisker deprived (WD) mice, compared to 0.85 ± 0.9 in control mice of the same age ($P < 0.05$; Fig. 1*D,E*). Importantly, the input/output slope of P19 WD mice was indistinguishable from those of young, P12 control mice ($P = 0.59$, Fig. 1*F*). These results suggest that a developmental increase in the CA3-CA1 input/output (Fig. 1*B–F*; Dumas and Foster 1995; Liao and Malinow 1996; Hsia et al. 1998) is occluded by prolonged whisker deprivation. The observed deprivation-induced reduction in the input/output relationship may result from a decrease in synaptic strength of CA3-CA1 connections as a compensatory response to the initial increase in the CA3-CA1 synaptic activity following the first 36 h of deprivation.

To examine whether the observed synaptic changes relate to deprivation-induced stress, we evaluated the effect of whisker deprivation on systemic corticosterone levels and stress/anxiety-related behavior of mice using the open field test. Basal serum corticosterone levels were not affected at 3 different time points along the period of deprivation: 1, 5, and 11 days (Fig. 1*G*). Additionally, whisker deprivation had no anxiogenic effect on open-field exploration: no differences between control and deprived mice were evident in traveled distance, number of entries to the center, and in the percent of time spent in the center of the open field (Fig. 1*H*). These outcomes indicate that stress is unlikely to be the mediator of deprivation-induced synaptic changes in the hippocampus of young mice.

Whisker Deprivation Impairs the Developmental Increase in Synapse Release Probability

To determine whether weakening of the presynaptic basal glutamate release may contribute to CA3-CA1 depression following prolonged, 9 ± 2 days of deprivation, we first used whole-cell

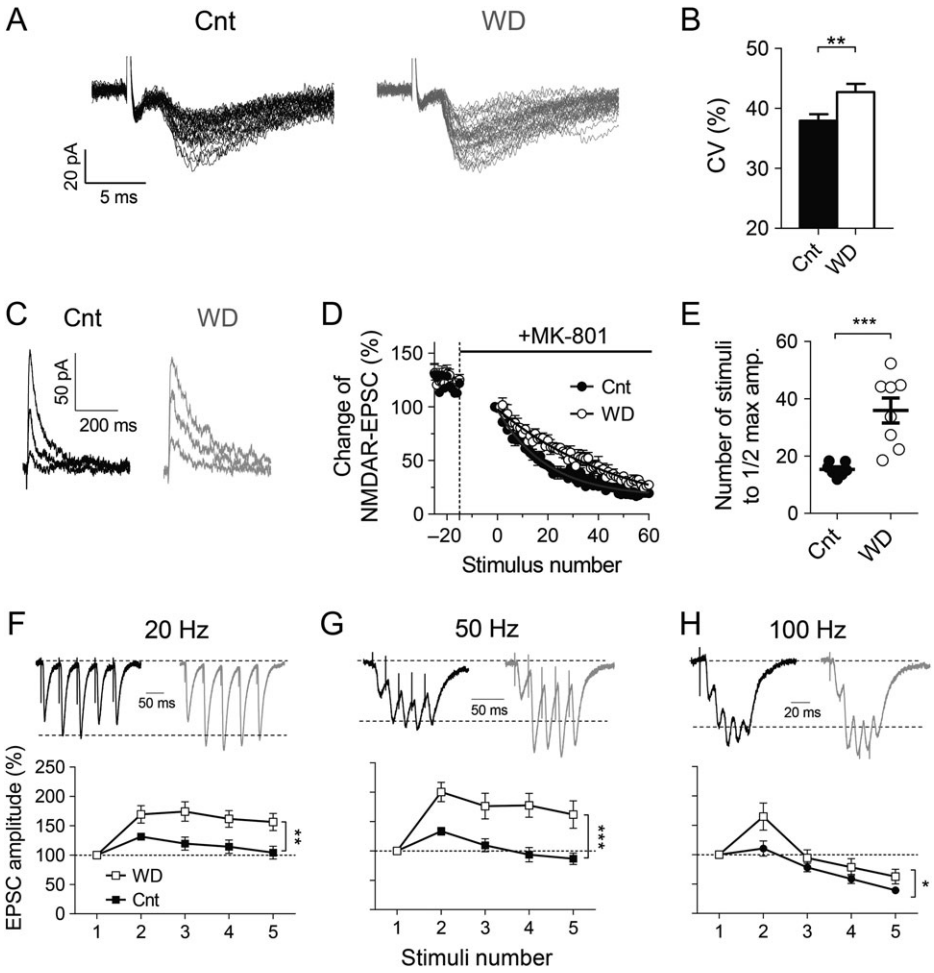

Figure 2. Whisker deprivation decreases the probability of vesicle release and induces an increase in short-term synaptic facilitation in CA3-CA1 connections. (*A*) Representative traces of Cnt and WD CA1 EPSCs in response to minimal stimulation. (*B*) CV of EPSC amplitude evoked by minimal stimulation (WD $N = 6$, $n = 18$, Cnt $N = 6$, $n = 19$; $P = 0.009$). (*C*) Representative traces of MK-801 mediated block of NMDAR-EPSCs in the 1st, the 20th, and the 50th trace in Cnt and WD mice. (*D*) Average decay in NMDAR-EPSC amplitude for Cnt ($n = 7$, $N = 5$) and WD ($n = 8$, $N = 5$) conditions. Decays are normalized to the amplitude of the first EPSC in MK-801 and fit to single exponential (solid lines). (*E*) Summary of the MK-801 effect on the stimuli number required to reach half of the NMDAR-EPSC amplitude (the same data as in B, $P = 0.0008$). Unpaired 2-tailed *t*-test. (*F–H*) Facilitation in response to repeated stimulation is higher in WD mice at frequencies of 20 Hz ($n = 8$, $N = 4$ for Cnt, $n = 8$, $N = 5$ for WD; $F_{1,14} = 11.85$, $P = 0.004$), 50 Hz ($n = 11$, $N = 6$ for Cnt, $n = 9$, $N = 6$ for WD; $F_{1,18} = 16$, $P = 0.0009$), and 100 Hz ($n = 14$, $N = 8$ for Cnt, $n = 9$, $N = 5$ for WD; $F_{1,21} = 4.9$, $P = 0.039$). Each burst contains 5 action potentials; inter-spike interval, 50 ms (*F*), 20 ms (*G*), and 10 ms (*H*); inter-burst interval was 30 s for 20 Hz and 60 s for 50 and 100 Hz bursts. Traces were normalized to the first peak in the burst. Upper dashed line represents the baseline, while the lower dash line represents the peak of the second amplitude in Cnt mice. Bottom: Average relative amplitudes of EPSCs within the burst, normalized to the first peak. Two-way ANOVA with repeated measurements (*P* values for the effect of deprivation are shown in the graphs: $^*P < 0.05$, $^{**}P < 0.01$, $^{***}P < 0.001$. Interaction with stimulus number is non-significant for all the conditions). Error bars represent s.e.m.

patch clamp recordings to record EPSC in the CA1 pyramidal neurons evoked by a minimal stimulation of a putative SC axon (Slutsky et al. 2010). Figure 2A shows individual traces and EPSC amplitude analysis from a typical recording of a putative single synaptic release site in control versus WD mice. CV of EPSC amplitudes was higher in WD mice (Cnt 37.9 ± 1.1%, WD 42.7 ± 1.4%, $P = 0.009$, Fig. 2B), supporting the interpretation that whisker disuse impairs developmental increase in release probability in CA3-CA1 synaptic connections (Dumas and Foster 1995; Bagley and Westbrook 2012).

As application of CV to determine release probability involves several assumptions, such as nearly all variances are presynaptic, which cannot be verified directly (Clements 2003). Therefore, we applied other independent methods to estimate release probability of synapses by calculating the rate of MK801 block of the NMDA receptor (NMDAR) and the degree of short-term facilitation. To analyze the rate at which the NMDAR open channel blocker MK-801 inhibits evoked excitatory postsynaptic currents mediated by NMDARs (NMDAR-EPSCs) in CA3-CA1 synapses of control and WD mice (Hessler et al. 1993; Rosenmund et al. 1993), we established a stable NMDAR response at +40 mV, then stimulation was stopped and MK-801 (40 μM) was bath-applied. After allowing for MK-801 to equilibrate at NMDARs in the slice, the SC stimulation was resumed. The amplitude of NMDAR-EPSCs was reduced by ~20% from the time of MK-801 application to the first stimulus due to spontaneous activity. The stimulation in the presence of MK-801 caused a rapid progressive block of the amplitude of NMDAR-mediated EPSCs (Fig. 2C) owing to the increasing number of receptors that became irreversibly blocked after use. The progressive block of NMDAR-EPSCs evoked each 20 s was well fitted by a single exponential, displaying 15.4 ± 0.9 stimuli required to reach half maximal amplitude in control mice (Fig. 2D,E). NMDAR-EPSCs exhibited 2.3-fold slower rate of MK-801 blockade in CA3-CA1 synapses of WD mice (35.92 ± 4.327 stimuli, $P = 0.0008$, Fig. 2C–E), providing an additional confirmation that long-term deprivation alters the presynaptic maturation.

Finally, we tested whether deprivation-induced reduction in the probability of glutamate release at the SC boutons may result in enhanced synaptic facilitation. This assumption is based on an inverse correlation between probability of neurotransmitter release and synaptic facilitation (Dobrunz and Stevens 1997; Tsodyks and Markram 1997; Zucker and Regehr 2002). To examine the influence of whisker deprivation on short-term synaptic plasticity, we recorded AMPAR-mediated EPSCs at −60 mV in CA1 pyramidal neurons, while stimulating the SCs by bursts composed of 5 stimuli at 20, 50, and 100 Hz (Fig. 2F–H). A 2-way ANOVA comparing the effects of deprivation and stimulus number during bursts, revealed a significant increase in synaptic facilitation by deprivation for 20 Hz burst ($F_{1,14} = 11.85$, $P = 0.004$), while indicating no interaction between deprivation and stimulus number during the burst ($F_{3,42} = 0.31$, $P = 0.82$). This indicates that, for WD mice, facilitation in CA3-CA1 connections is enhanced equally throughout the burst relative to littermate controls. The same pattern holds for 50 Hz ($P = 0.0009$) and 100 Hz ($P = 0.039$) burst stimuli. Similar results were observed when patch clamp recordings were performed at near physiological temperature (32 °C, see Supplementary Fig. 1A–C). In an effort to assess the robustness of the results obtained by our experimental design, we performed whisker deprivation in another strain of mice, C57BL/6 J, exhibiting higher degree of synaptic facilitation at CA3-CA1 synapses in comparison to BALB/c mice (see Supplementary Fig. 1D–F). Importantly, whisker deprivation enhanced synaptic facilitation in CA3-CA1 connections of C57BL/6 J mice as well, although the effect was more pronounced at higher burst frequencies, leaving synaptic dynamics at 20 Hz stimulation unaffected. Altogether, these results suggest that tactile experience in early life impacts the developmental program that up-regulates release probability, thus modulating the filter properties of CA3-CA1 hippocampal synapses.

Deprivation-Induced Increase in Synaptic Facilitation Remains Stable After Whisker Regrowth

To examine the stability of deprivation-induced synaptic changes, we allowed for 3 weeks of whiskers regrowth and postponed recordings of synaptic facilitation to P40 ± 2 (Fig. 3A). As evident from the data illustrated in Figure 3B,D, short-term synaptic facilitation at 50 and 100 Hz did not recover 2–3 weeks following deprivation, suggesting that tactile disuse during early development induced long-lasting changes in synaptic vesicle release at the CA3 boutons. Notably, neither basal corticosterone levels (Fig. 3E), nor anxiety-related behavioral outputs (Fig. 3F,G) were altered after 3 weeks of whisker regrowth. In particular, percentage of time spent in the center or the total traveled distance, measured in an open field (Fig. 3F), and the percent of time spent in the open arms or the percent of entries to the open arms measured in an elevated plus-maze (Fig. 3G) were similar between control and deprived groups. These data indicate that deprivation-induced modifications of hippocampal synapses in young adult mice have occurred via stress-unrelated mechanisms.

WD Alters the Fraction of Silent Synapses, the NMDAR Subunit Composition and AMPA/NMDA Ratio at CA3-CA1 Synapses

As whisker deprivation interferes with normal development of AMPAR-mediated EPSC, we tested whether the percentage of silent synapses may change following WD. Therefore, we compared the trial-to-trial coefficient of variation (CV) of AMPAR- and NMDAR-mediated EPSCs, isolated at −65 and +40 mV, respectively, and measured on the basis of their distinct kinetics (Fig. 4A). The CV is generally inversely proportional to the number of functional synapses and their release probability (Kullmann 1994). Thus, for a given set of synapses mixed with silent (NMDAR only) and non-silent synapses, the total number of NMDAR-containing synapses (measured at +40 mV) should be greater than the number of AMPAR-containing synapses (measured at −65 mV; NMDAR-only synapses are blocked by Mg^{2+} at this voltage), resulting in reduced ratio of CV of NMDAR (CV_{NMDAR}) EPSCs to CV of AMPAR (CV_{AMPAR}) EPSCs. After 9 ± 2 days of whisker deprivation, the CV_{NMDAR}/CV_{AMPAR} ratio was decreased in CA3-CA1 synapses ($P = 0.0004$, Fig. 1B). These results indicate that tactile disuse impairs normal development of CA3-CA1 synapses, characterized by a decrease in the fraction of SC silent synapses (Durand and Konnerth 1996; Hanse et al. 2013).

Next, we tested whether deprivation affects the synaptic AMPA-to-NMDA ratio (AMPA/NMDA). Indeed, the AMPA/NMDA ratio, estimated at +40 mV (see methods for details), was reduced by deprivation (Fig. 4C,D; $P < 0.01$). It is worth noting that the calculated AMPA/NMDA ratio may be underestimated since the low pass filtering properties of pyramidal neurons cause the faster AMPAR-mediated EPSC component to be filtered more than the slower NMDAR-mediated EPSC component. Given the developmental increase in the AMPA/NMDA ratio in CA3-CA1 synapses (Hsia et al. 1998; Bagley and Westbrook 2012), whisker deprivation may intervene with the maturation of synaptic AMPA and NMDA receptors in the hippocampus.

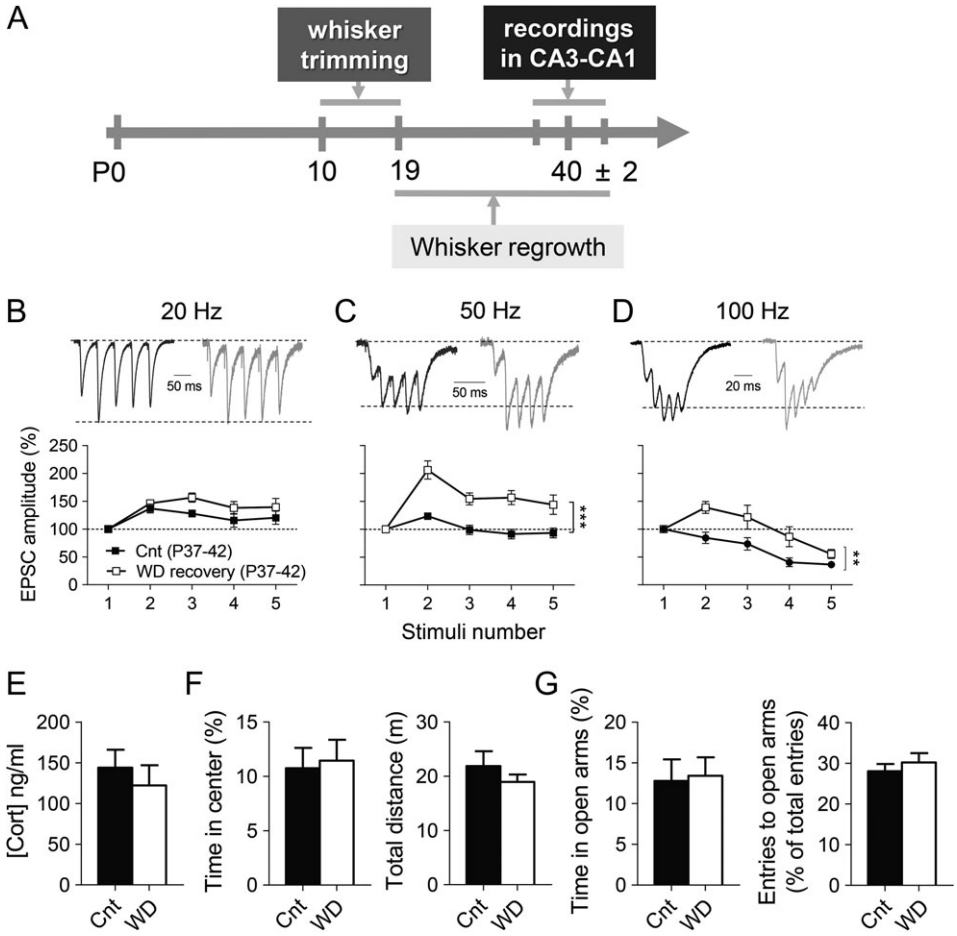

Figure 3. Whisker deprivation early in life induces a lasting increase in short-term synaptic facilitation in CA3-CA1 connections without altering stress-related characteristics. (*A*) Experimental design. Whiskers were bilaterally trimmed from P10 to P19. The whiskers were then allowed to regrow for ~3 weeks, and recordings were made at P40 ± 2. (*B–D*) Facilitation is higher in WD mice at 50 Hz ($n = 14$, $N = 6$ for Cnt, $n = 10$, $N = 5$ for WD; $F_{1,22} = 25$, $P < 0.0001$) and 100 Hz ($n = 11$, $N = 6$ for Cnt, $n = 8$, $N = 5$ for WD; $F_{1,17} = 9.3$, $P = 0.007$), while was not altered at 20 Hz ($n = 8$, $N = 5$ for Cnt, $n = 9$, $N = 5$ for WD; $F_{1,15} = 2.9$, $P = 0.11$) stimulation frequencies. Each burst contains 5 action potentials; inter-spike interval, 50 ms (*B*), 20 ms (*C*), and 10 ms (*D*); inter-burst interval was 30 s for 20 Hz and 60 s for 50 and 100 Hz bursts. Traces were normalized to the first peak in the burst. Upper dashed line represents the baseline, while the lower dash line represents the peak of the second amplitude in Cnt mice. Bottom: Average relative amplitudes of EPSCs within the burst, normalized to the first peak. Two-way ANOVA with repeated measurements (*P* values for the effect of deprivation are shown in the graphs: $^{**}P < 0.01$, $^{***}P < 0.001$. Interaction with stimulus number is non-significant for all the conditions). (*E*) Basal plasma corticosterone levels of Cnt and WD mice at P50 (WD $N = 8$, Cnt $N = 7$, $P = 0.89$). (*F*) No change has been found between WD ($N = 34$) and Cnt ($N = 29$) in the open field test: the 2 groups spent the same amount of time in the center of the arena (left, $P = 0.8$) and had traveled the same distance (right, $P = 0.3$). (*G*) No change has been found between WD ($N = 18$) and Cnt ($N = 17$) in the elevated plus-maze test: the 2 groups spent the same percent of time in the open arms (left, $P = 0.85$) and entered the same number of times to the open arms (right, $P = 0.077$). Unpaired 2-tailed *t*-test (*E–G*). Error bars represent s.e.m.

Then, we examined whether whisker deprivation affects the subunit composition of NMDARs in CA3-CA1 synapses, exhibiting reduction in the NR2B-containing receptors during the third week of hippocampal development (Sans et al. 2000). These developmental changes are accompanied by an acceleration of the NMDAR-EPSC decay and a decrease in sensitivity to ifenprodil, a selective NR2B blocker (Kirson and Yaari 1996; Bellone and Nicoll 2007). To compare the decay of NMDAR-EPSC between CA3-CA1 connections in control and WD mice, we recorded evoked EPSCs at +40 mV. Interestingly, whisker deprivation increased the NMDAR-EPSC decay from 126 ± 6 to 151 ± 5.5 ms (Fig. 4*E*,*F*; $P = 0.005$). The prolonged decay of NMDAR-EPSC indicates an increase in the number of NR2B-containing NMDARs. To test this possibility, we determined in control versus deprived mice the sensitivity of NMDAR-EPSC to 3 μM ifenprodil, a concentration producing only negligible effect on P/Q-type calcium channels (Delaney et al. 2012). Indeed, whisker deprivation enhanced the ifenprodil-sensitivity of NMDAR-EPSC (Fig. 4*E*). On average, ifenprodil reduced the total charge transfer of NMDAR-EPSC in CA3-CA1 synapses by ~49% in WD, while only by ~34% in control mice (Fig. 4*G*; $P = 0.005$). Thus, depriving mice of vibrissae stimuli impairs the developmental NR2B/NR2A switch in CA3-CA1 hippocampal connections.

In addition to NMDARs, AMPARs undergo the subunit composition during the second week of development. Namely, the expression of the GluA2 subunit is increased in the hippocampus (Monyer et al. 1991), leading to a reduction in an inward rectification due to voltage-dependent block of the channel pore by polyamines (e.g., spermine) at positive membrane potentials (Isaac et al. 2007). To examine if whisker experience contributes to GluA2 enrichment, we monitored the rectification index of AMPAR-mediated EPSCs in slices of WD versus control animals. Whole-cell patch clamp recordings of CA1 neurons were performed using an intracellular solution that contains spermine (Plant et al. 2006). Pharmacologically isolated AMPAR-mediated EPSCs, evoked by stimulation of the

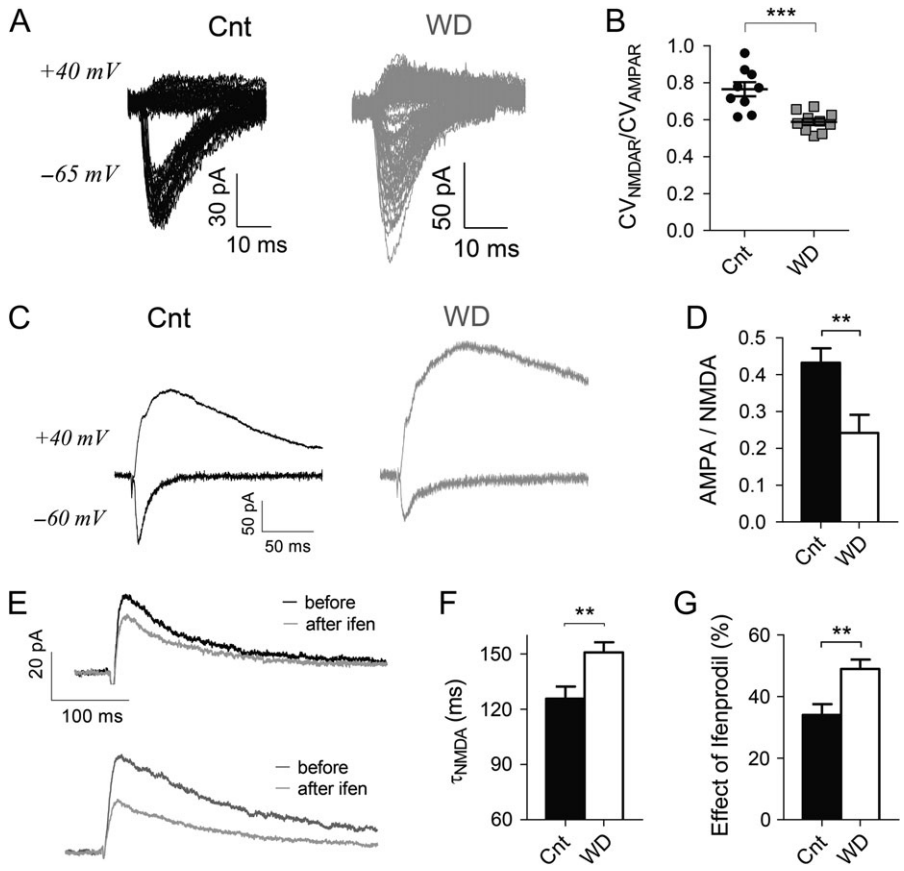

Figure 4. Modification of the postsynaptic properties following whisker deprivation in CA3-CA1 synapses. (*A*) AMPAR-EPSCs recorded at −65 mV and NMDAR-EPSCs recorded at +40 mV (in the modified ASCF, containing gabazine, 4 mM Ca^{2+} and 4 mM Mg^{2+}) in slices of Cnt (black) and WD (gray) mice. (*B*) Summary of the data, showing lower CV_{NMDAR}/CV_{AMPAR} in WD (WD and Cnt $n = 9–10$, $N = 5$; $P = 0.0004$). (*C*) Representative EPSCs recorded by regular stimulation at −60 and +40 mV in slices of Cnt (black) and WD (gray) mice. (*D*) AMPA/NMDA ratio was lower ($P = 0.006$) in WD ($n = 11$, $N = 6$) than in Cnt ($n = 11$, $N = 5$) mice. (*E*) Representative NMDAR-EPSCs recorded at +40 mV in slices of Cnt (black) and WD (gray) mice before and 10 min after application of ifenprodil (3 μM). (*F*) Deprivation prolonged the decay time of NMDAR-EPSCs (Cnt $n = 23$, $N = 11$; WD $n = 33$, $N = 12$; $P = 0.005$). (*G*) Deprivation enhanced the effect of ifenprodil on the charge transfer of NMDAR-EPSCs ($n = 10$, $N = 7$; $P = 0.005$). ***$P < 0.001$, **$P < 0.01$. Unpaired 2-tailed *t*-test. Error bars represent s.e.m.

SCs, did not demonstrate any difference in AMPAR I-V relationship between WD and control mice, resulting in similar AMPAR rectification index (see Supplementary Fig. 2; $P > 0.2$). These results indicate that, unlike the NMDAR subunit composition, the developmental increase in the GluA2/GluA1 ratio at CA3-CA1 synapses does not depend on sensory experience.

Deprivation Downregulates Quantal Amplitude in CA1 Neurons, but not in CA3-CA1 Synapses

We next explored whether 9 ± 2 days of deprivation induces a modification of quantal excitatory synaptic transmission. Therefore, we compared miniature AMPAR-mediated EPSCs (mEPSCs) in CA1 neurons of WD versus control mice. Whisker deprivation did not alter mEPSC frequency (Fig. 5A,B; $P = 0.29$, K–S test), which might indicate differential regulation of spontaneous and evoked EPSCs (Kavalali 2015) by sensory deprivation. In contrast, deprivation triggered a ~20% reduction in mEPSC amplitude (Fig. 3A,C; $P < 0.0001$, K–S test).

As CA1 pyramidal neurons receive multiple inputs, including the SC, the temporoammonic (TA) and the input onto stratum oriens, we asked whether the change in mEPSC amplitude is caused by a reduction in quantal size in the SC connections. To answer this question, we analyzed the mean amplitude of the successful AMPAR-mediated EPSCs evoked by minimal stimulation of a SC axon. No differences were observed between minimally evoked mean EPSC amplitudes in WD and control mice (Mean amplitude in Cnt: 22.33 ± 1.53 pA; in WD: 23.17 ± 1.28 pA Fig. 5D; $P = 0.68$). Likewise, AMPAR-mediated EPSCs evoked by pressure application of L-glutamate to apical stratum radiatum dendrites elicited an inward current with a similar dependency on the duration of glutamate puff for both WD and control mice (Fig. 5E,F; $P > 0.05$). As glutamate application activates multiple synapses at the CA1 dendrites, we quantified spine density at the apical dendrites (100–150 μm from soma) in the recorded neurons. Utilizing 2-photon-microscopy of neurons labeled with fluorescent AlexaFluor-488 dye added to the intracellular solution, no differences had been found in spine density between the 2 groups (Fig. 5G,H; $P = 0.87$). Collectively, these results indicate that the CA3-CA1 synapses do not contribute to deprivation-induced decrease in mEPSC amplitude at the CA1 neurons.

Sensory Deprivation Reduces Intrinsic Excitability of CA3, but not CA1 Neurons

Next, we explored whether the reduction in CA3 excitability contributes to the CA3-CA1 depression. Therefore, we

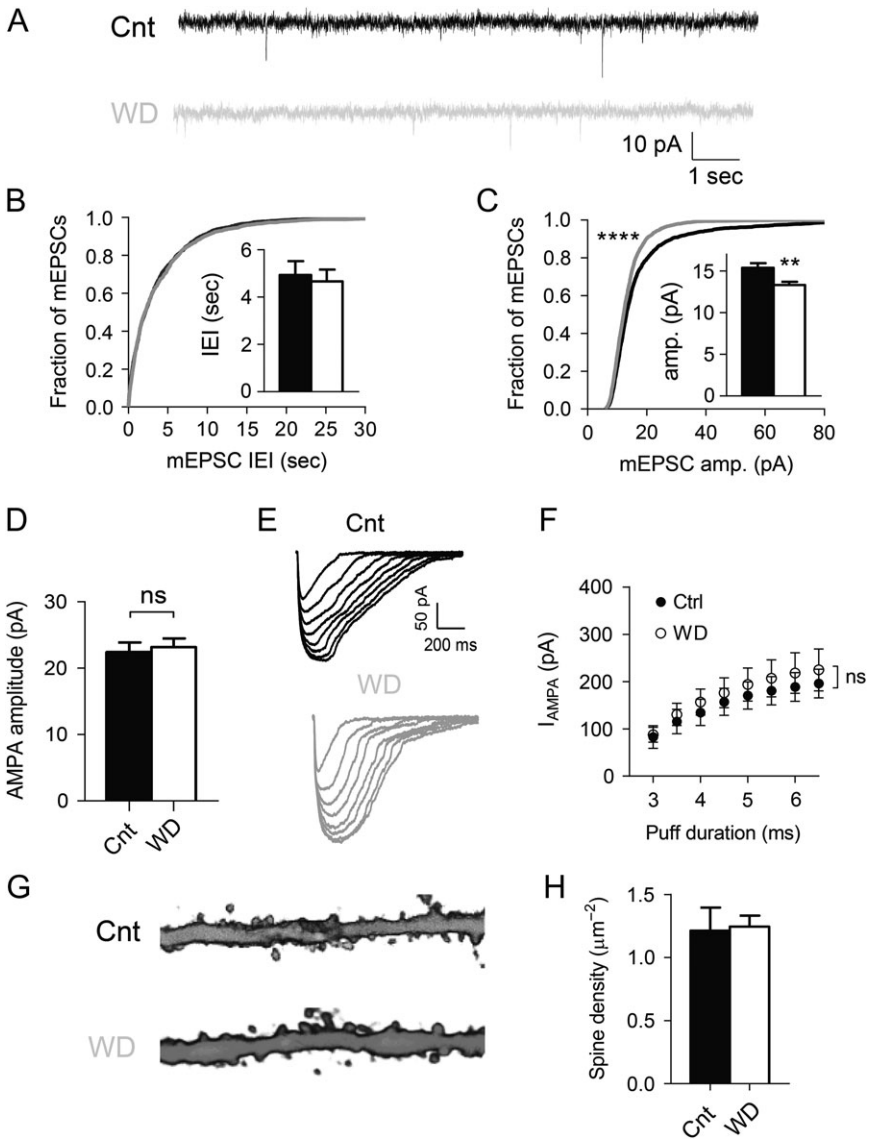

Figure 5. Whisker deprivation decreases mEPSC quantal amplitude of CA1 neurons without affecting postsynaptic AMPAR-mediated response in CA3-CA1 connection. (*A*) Representative traces of mEPSCs for Cnt and WD conditions. (*B*) Cumulative histogram of mEPSC inter-event intervals (IEI) showing similar distribution between WD (n = 15, N = 7) and Cnt (n = 14, N = 7) conditions. Insert: data summary. Mean mEPSC frequency is not altered by deprivation (K–S test, P = 0.29; unpaired t-test, P = 0.72). K–S test for distribution histogram and unpaired 2-tailed t-test for mean (amplitude/IEI) in each cell. (*C*) Cumulative distributions of mEPSC amplitudes in WD (n = 15, N = 7) and Cnt (n = 14, N = 7) mice. The mean of mEPSC amplitude decreased (K–S test, $P < 0.0001$; unpaired t-test, $P < 0.01$) from 15.4 to 13.3 pA following whisker deprivation. Insert: data summary. (*D*) AMPAR-mediated EPSC amplitude evoked by minimal stimulation of CA3-CA1 synapses shows no change following WD (Cnt n = 19, N = 6; WD n = 18, N = 6; P = 0.68). (*E*) Representative traces of the AMPA current induced by pressure application of 5 mM L-glutamate for 3–6.5 ms (0.5 ms increment) in Cnt (upper traces) and WD mice (lower traces). (*F*) Averaged amplitude of AMPA currents induced by the local application of glutamate with incremented duration (3–6.5 ms) in Cnt (n = 14, N = 6) and WD (n = 13, N = 5) mice. (*G*) Representative 2-photon images of apical CA1 dendrites. (*H*) Quantitative analysis of spine density on apical CA1 dendrites shows no difference following deprivation (Cnt n = 5, 15 images; WD n = 6, 20 images; P = 0.87). $^{**}P < 0.01$, $^{***}P < 0.001$. Unpaired 2-tailed t-test. Error bars represent s.e.m.

measured the effect of deprivation on the electrophysiological properties of CA3 pyramidal neurons. Action potentials were elicited in response to somatic current injections ranging from −40 to +300 pA, starting from resting membrane potential, in the presence of synaptic blockers (Fig. 6A). Notably, sensory deprivation decreased the frequency of action potentials in response to incremental current injections (Fig. 6A,B; $F_{1,27}$ = 8.5, P = 0.007). Moreover, whisker deprivation lowered the CA3 cell input resistance by ~15% (Fig. 6C; P = 0.018) when measured in proximity of the resting membrane potential, which was not altered (Fig. 6D; P = 0.73). The threshold for generating of single action potential (Fig. 6E; P = 0.125), as well as action potential amplitude (Fig. 6F; P = 0.62) were not significantly modified. Importantly, the excitability of CA3 neurons did not show developmental changes during the deprivation period (P12 vs. P20, see Supplementary Fig. 3). Thus, deprivation appears to actively modify the excitability of neurons in young mice. In contrast to CA3, CA1 pyramidal neurons were not sensitive to whisker deprivation, displaying similar active and passive excitability properties to controls (see Supplementary Fig. 4). Taken together, these

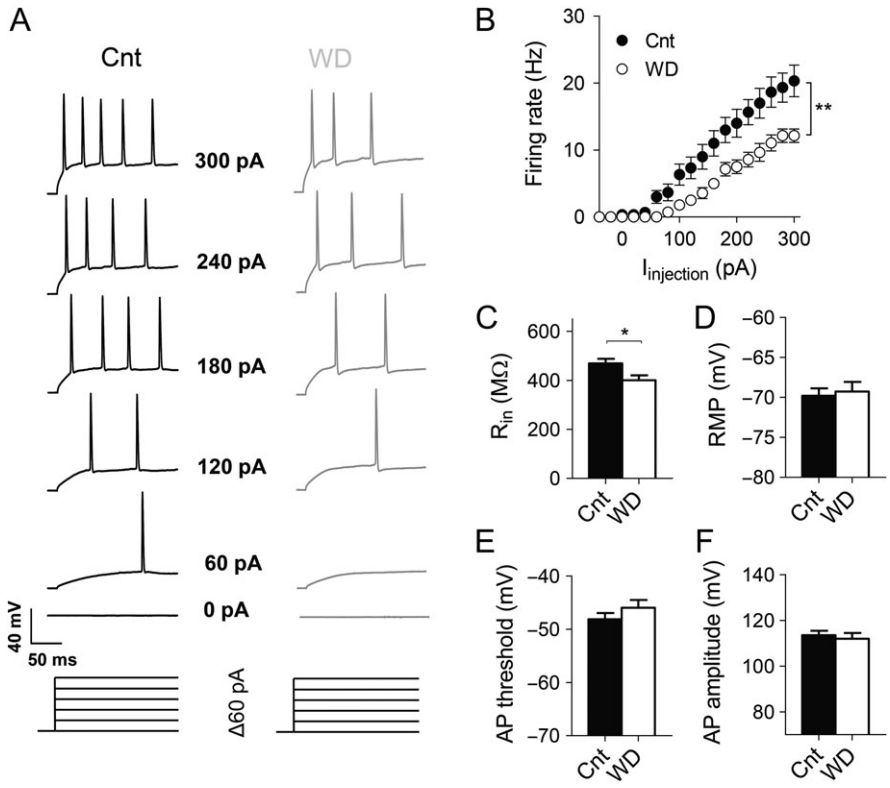

Figure 6. Whisker deprivation decreases the excitability of CA3 pyramidal neurons. (*A*) Representative traces of voltage responses evoked by 20 pA step of current injections in CA3 neurons of WD and Cnt mice, elicited from resting membrane potential (~-70 mV). (*B*) Deprivation triggered a decrease in *F-I* relationship (Cnt $n = 15$, $N = 7$; WD $n = 14$, $N = 5$; $F_{1,27} = 8.46$, $P = 0.0072$; 2-way ANOVA with repeated measurements). (*C*) Deprivation decreased input resistance (R_{in}, Cnt $n = 15$, $N = 6$; WD $n = 13/4$; $P = 0.018$). (*D*) Deprivation did not alter resting membrane potential (RMP, Cnt $n = 10$, $N = 6$; WD $n = 10$, $N = 5$; $P = 0.73$). (*E*) Deprivation did not affect threshold of action potential (Cnt $n = 15$, $N = 6$; WD $n = 13$, $N = 5$; $P = 0.125$). (*F*) Deprivation did not affect amplitude of action potential (Cnt $n = 15$, $N = 6$; WD $n = 13$, $N = 5$; $P = 0.62$). *$P < 0.05$, **$P < 0.01$. Unpaired 2-tailed *t*-test (*E–F*). Error bars represent s.e.m.

results demonstrate that whisker deprivation selectively reduces intrinsic excitability of CA3 pyramidal neurons.

Deprivation in Adult Mice does not Alter the Synaptic Strength of the CA3-CA1 Connections or its Synaptic Facilitation, but Reduces CA3 Excitability

The period of whisker deprivation studied above (P10 to P19 ± 2) overlaps with a critical period of plasticity of the barrel cortex and a period of active development for CA3-CA1 synapses. In particular, synaptic strength at CA3-CA1 connections increases till the fourth postnatal week (Fig. 1*F*) and short-term synaptic facilitation undergoes a pronounced developmental reduction from the second to the third postnatal week, while stabilizing from the fourth week (see Supplementary Fig. 5). Thus, whisker trimming may lead to synaptic weakening by impairing the normal development of CA3-CA1 synapses. If this is the case, whisker deprivation during the mature CA3-CA1 period should not augment synaptic facilitation or change the input/output curve of the synapses. Thus, we started the WD in P28 and recorded from slices of P40 ± 2 mice (Fig. 7*A*). Indeed, whisker deprivation during this postnatal period did not significantly affect input/output curve (Fig. 7*B*; $P = 0.87$) or short-term plasticity in CA3-CA1 synapses (Fig. 7*C–E*; $P > 0.2$), indicating that there is a sensitive period during which tactile experience shapes presynaptic properties of CA3 boutons.

In contrast to the presynaptic modifications, intrinsic excitability of CA3 neurons was invariant during the period of deprivation (see Supplementary Fig. 3). Therefore, we asked whether whisker deprivation may regulate CA3 excitability in adult mice after the end of the critical period of barrel cortex plasticity. Interestingly, whisker deprivation from P28 to P40 ± 2 resulted in a significant reduction in the firing rate to current injection relationship ($F_{1,19} = 8.6$, $P = 0.0085$; Fig. 7*F,G*), without altering the input resistance, action potential threshold or amplitude (see Supplementary Fig. 6). Thus, whisker deprivation in adult mice leads to hypoexcitability of CA3 pyramidal neurons without altering AMPAR-mediated synaptic properties in the CA3-CA1 connections.

Discussion

Understanding how sensory experience shapes synaptic dynamics in hippocampal circuits is fundamental for delineating the role of the hippocampus in cognitive functions. The major finding of this study is that the history of sensory experience in early postnatal life shapes synaptic and intrinsic properties of hippocampal circuits. Namely, long-term (9 ± 2 days) whisker deprivation depresses the input/output relationship in CA3-CA1 synapses through multiple mechanisms, reduces the CA3 intrinsic excitability, boosts short-term synaptic facilitation during high-frequency spike bursts and alters the subunit composition of synaptic NMDARs and the AMPA/NMDA ratio. These changes should profoundly impact synaptic and neuronal computations performed by the hippocampus.

During the last decades, a combination of theoretical and empirical studies have pointed to the existence of emerging

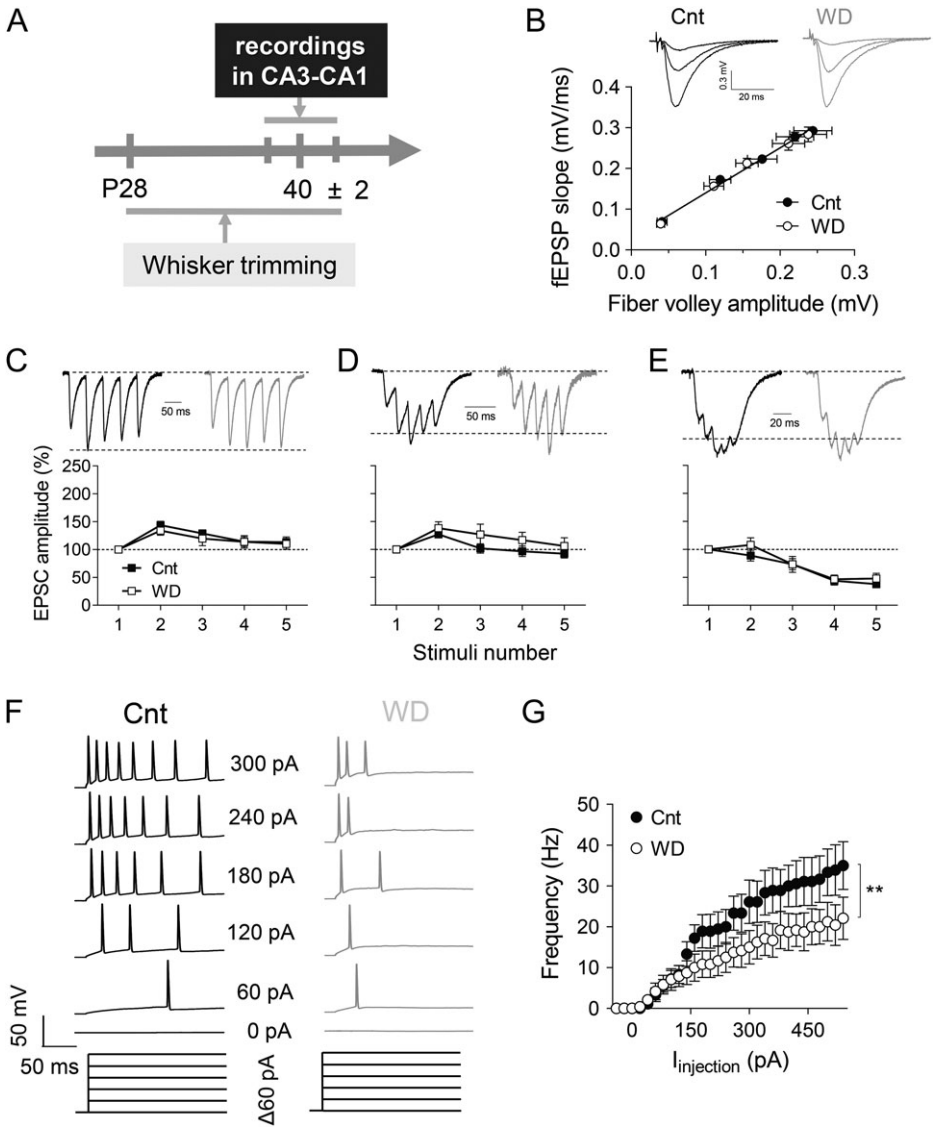

Figure 7. Whisker deprivation in young adult mice does not induce a change in synaptic strength or an increase in short-term synaptic facilitation in CA3-CA1 connections, but decreases firing rate of CA3 neurons. (*A*) Experimental design. Deprivation from P28 to P40 ± 2, recordings at P40 ± 2. (*B*) Top: Representative fEPSP recordings in different stimulation intensities (20, 50, and 100 μA; black—Cnt, grey—WD). Bottom: Input-output relationship between the amplitude of fiber volley and the slope of fEPSP for gradually increasing stimulation intensities in CA3-CA1 connections was unaltered by WD in young adult mice (Cnt $n = 10$, $N = 5$; WD $n = 11$, $N = 5$; $P = 0.87$). (*C–E*) Short-term synaptic plasticity at the CA3-CA1 connections was not affected by WD in young adults. Top: Representative recordings of EPSCs at −60 mV in Cnt (black) and WD (gray) mice evoked by a burst: each burst contains 5 action potentials; inter-spike interval, 50 ms (*C*), 20 ms (*D*), and 10 ms (*E*); inter-burst interval was 30 s for 20 Hz and 60 s for 50 and 100 Hz bursts. Traces were normalized to the first peak in the burst. Upper dashed line represents the baseline, while the lower dash line represents the peak of the second amplitude in Cnt mice. Bottom: Average relative amplitudes of EPSCs within the burst, normalized to the first peak. Facilitation is not affected by whisker deprivation at 20 Hz ($n = 11$, $N = 7$ for Cnt and WD; $F_{1,20} = 0.23$, $P = 0.64$), 50 Hz ($n = 16$, $N = 7$ for Cnt, $n = 12$, $N = 7$ for WD; $F_{1,26} = 2.0$, $P = 0.17$), and 100 Hz ($n = 13$, $N = 7$ for Cnt, $n = 12$, $N = 7$ for WD; $F_{1,23} = 0.64$, $P = 0.43$). (Interaction with stimulus number is non-significant for all the conditions). (*F*) Representative traces of voltage responses evoked by 20 pA step of current injections in CA3 neurons of WD and Cnt mice, elicited from resting membrane potential (~−70 mV). (*G*) Deprivation triggered a decrease in *F-I* relationship (Cnt $n = 10$, $N = 4$; WD $n = 11$, $N = 5$; $F_{1,19} = 8.6$, $P = 0.0085$, 2-way ANOVA with repeated measurements). **$P < 0.001$. Unpaired 2-tailed *t*-test. Error bars represent s.e.m.

principles underlying processing of sensory information in the primary sensory cortices (Petersen Carl and Crochet 2013). Surprisingly, we know very little about how sensory information is processed in the hippocampus. A pioneering study by Nicolelis group (Pereira et al. 2007) demonstrates that trigeminal inputs from the whiskers reach the CA1 hippocampal region through the thalamic ventral posteromedial nucleus (VPM) and the primary somatosensory cortex (S1), evoking increase in firing rate in ~52% of CA1 neurons in freely behaving rats. In this study, tactile responses in the CA1 were completely blocked by simultaneous pharmacological inactivation of VPM and S1, suggesting that tactile responses in the CA1 depend on the integrity of somatosensory lemniscal pathway. CA1 neurons form a representation of textures in a context (Itskov et al. 2011) and vigilance state (Vinogradova 2001; Pereira et al. 2007) dependent manner. For example, somatosensory stimulation in urethane-anesthetized

rats suppresses neuronal firing in the CA1 region (Bellistri et al. 2013), while it augments firing of CA1 neurons in awake rats (Pereira et al. 2007).

Whisker Deprivation Induces Reconfiguration of CA3-CA1 Synapses

Although the majority of CA1 hippocampal neurons respond to tactile information, how tactile experience regulates functional properties of hippocampal neurons remains unknown. Our study demonstrates that 9 ± 2 days of bilateral whisker trimming early in life depresses neuronal and synaptic activity in the CA3-CA1 connections through multiple mechanisms. First, it triggers a decrease in excitability in presynaptic CA3 neurons. Second, it reduces the probability of synaptic vesicle release in the CA3-CA1 connections. Third, it causes an increase in the fraction of postsynaptically silent synapses. Thus, in addition to extensively studied L4 to L2/3 synaptic depression in the primary somatosensory cortex (Fox 2002; Feldman 2009), whisker deprivation causes a pronounced depression in the CA3-CA1 synapses, the last step in the hippocampal trisynaptic circuit.

How does refinement of synaptic circuitry during hippocampal development depend upon sensory experience? On the one hand, tactile disuse diminishes CA3 excitability and quantal mEPSC amplitude of CA1 neurons, most likely due to the postsynaptic changes in TA or stratum oriens synapses. These characteristics are not regulated by development (see Supplementary Fig. 3; Hsia et al. 1998), suggesting that sensory experience actively strengthens CA3 excitability and excitatory quantal amplitude of CA1 neurons. On the other hand, developmental increase in several synaptic parameters, such as glutamate release probability (Dumas and Foster 1995), the AMPA/NMDA ratio (Hsia et al. 1998), and in the NR2A/NR2B ratio (Kirson and Yaari 1996; Bellone and Nicoll 2007), together with a decrease in the fraction of silent synapses (Durand and Konnerth 1996; Hanse et al. 2013) and short-term facilitation (Dumas and Foster 1995; deKay et al. 2006; Speed and Dobrunz 2008; Supplementary Fig. 5) is impaired by whisker deprivation in CA3-CA1 hippocampal synapses. Similar presynaptic (Bender et al. 2006; Cheetham and Fox 2011) and postsynaptic (Carmignoto and Vicini 1992; Philpot et al. 2001; Mierau et al. 2004; Funahashi et al. 2013) changes were observed following sensory deprivation during the development of primary sensory cortices, suggesting that sensory experience may regulate maturation of specific synaptic parameters across different brain regions.

While the effect of sensory deprivation on firing properties of the L2/3 of the EC—the main sensory gate providing direct input to the hippocampus—are awaiting to be investigated, our study demonstrates a sharp increase in the SC input/output during the first 36 h following whisker deprivation (Fig. 1*B*,*C*). An increase in the duration of deprivation to 9 ± 2 days results in a depression of CA3-CA1 synapses (Fig. 1*D*,*E*). The observed changes in synaptic and intrinsic properties following prolonged whisker deprivation may be a result of a homeostatic response to initial hyperactivity of the SC synapses following deprivation. Interestingly, studies in the primary visual cortex demonstrate multiple homeostatic adaptations expressed as a delayed increase in synaptic excitatory drive and in intrinsic excitability to initial depression induced by monocular deprivation (Maffei et al. 2004; Lambo and Turrigiano 2013). These changes have been proposed to maintain the mean firing rate of neurons at the set-point level of activity following deprivation (Hengen et al. 2013; Keck et al. 2013). Markedly, the SC input/output relationship following prolonged deprivation returns to the lower level, indistinguishable from the one characterizing the SC of young mice in the beginning of deprivation period (Fig. 1*F*). These results imply that developmental increase in the set-point level of activity in the CA3-CA1 hippocampal connections is not entirely preprogrammed, but is regulated by sensory experience.

How plastic are hippocampal neurons to tactile disuse after the end of critical period of barrel cortex plasticity? In adult mice, whisker deprivation significantly reduced CA3 intrinsic excitability, but did not alter the presynaptic CA3 function detected by changes in synaptic facilitation or the overall synaptic strength. These properties of CA3 neurons display differential regulation during P10–20 period of mouse development, coinciding with the barrel cortex critical periods. Namely, an enhancement of CA3 release probability (see Supplementary Fig. 5), but invariant CA3 excitability (see Supplementary Fig. 3) were observed during this developmental period. Thus, we propose that critical period of plasticity is not a unique property of neurons in the primary sensory cortices. Some features of hippocampal neurons, such as probability of vesicle release, are fine-tuned by sensory experience in sensitive period during early development. Conversely, the properties of hippocampal neurons that display stability during this time period, such as CA3 excitability, remain sensitive to the history of tactile experience throughout life.

Does whisker deprivation selectively promote synaptic facilitation in the SC pathway, or does it generally enhance facilitation in excitatory synapses of cortico-hippocampal circuitry? In particular, whether the TA pathway, connecting the L3 entorhinal cortex neurons and the distal dendrites of the CA1 neurons, responds to sensory deprivation? Interestingly, the medial TA path displayed enhanced synaptic facilitation following whisker deprivation, while the lateral TA path remained immune to the deprivation (see Supplementary Fig. 7). Based on these results, we conclude that whisker experience early in life limits short-term facilitation of hippocampal synapses in a pathway-specific manner. Future studies are needed to understand the mechanisms underlying this selectivity.

How do hippocampal synapses respond to different types of sensory deprivation? Unimodal sensory deprivation from birth causes cross-modal synaptic changes in synaptic properties in other primary sensory cortices, in addition to synaptic depression in the corresponding primary sensory cortex (Goel et al. 2006; Jitsuki et al. 2011; Zheng et al. 2014). Interestingly, our early work demonstrates that dark rearing during P8–35 period enhances synaptic facilitation in CA3-CA1 connections without altering synaptic depression in the primary visual cortex (Dolev et al. 2013). These results indicate that hippocampal synapses respond similarly to visual and tactile disuse. It remains to be seen how different sensory modalities regulate ongoing spiking patterns of single neurons and neuronal populations in the hippocampus.

Functional Significance

In the current work we characterized a basic relationship between sensory disuse and synaptic transmission in the hippocampus. Based on our findings, we suggest that sensory experience during early life constrains the plasticity in hippocampal synapses by strengthening basal synaptic transmission and shortening the duration of NMDAR-mediated currents. These results will serve as a foundation for future experiments investigating the interactions between sensory reality, represented by sensory information directly arriving from the entorhinal cortex, and the predictions that arrive from the internally stored representations in the CA3 network. Tuning

such comparative "match–mismatch" hippocampal computations by the history of sensory experience may impact detection of novel stimuli and associations (Lisman and Otmakhova 2001; Vinogradova 2001; Kumaran and Maguire 2009). As a failure in hippocampal sensory processing constitutes a pathophysiological hallmark of psychiatric disorders (Freedman et al. 1996), understanding the link between developmental sensory deficits and hippocampal plasticity may lead to new conceptual insights into the etiology of mental illness.

Supplementary Material

Supplementary material are available at *Cerebral Cortex* online.

Funding

This work was supported by the European Research Council starting grant (281403, IS), the Legacy Heritage Biomedical Program of the Israel Science Foundation (1195/14, IS), Israel Science Foundation (398/13, IS), Binational Science Foundation (2013244, IS) and the Marie Curie CIG grant (33458, SF). I.S. is grateful to Sheila and Denis Cohen Charitable Trust and Rosetrees Trust of the UK for their support.

Notes

We thank Dr. Ilan Lampl and all the lab members for fruitful discussions and Lior Bikovski for help with behavioral experiments. The behavioral experiments were carried out in the Hebrew University and in the Myers Neuro-Behavioral Core Facility of Tel Aviv University. H.M.P., C.L., and A.B. are grateful to Sagol School of Neuroscience of Tel Aviv University for the award of doctoral fellowships. This work was performed in partial fulfillment of the requirements for a Ph.D. degree by Hila Milshtein-Parush at the Sackler Faculty of Medicine, Tel Aviv University, Israel. *Conflict of Interest*: None declared.

References

Bagley EE, Westbrook GL. 2012. Short-term field stimulation mimics synaptic maturation of hippocampal synapses. J Physiol. 590:1641–1654.

Bellistri E, Aguilar J, Brotons-Mas JR, Foffani G, de la Prida LM. 2013. Basic properties of somatosensory-evoked responses in the dorsal hippocampus of the rat. J Physiol. 591: 2667–2686.

Bellone C, Nicoll RA. 2007. Rapid bidirectional switching of synaptic NMDA receptors. Neuron. 55:779–785.

Bender KJ, Allen CB, Bender VA, Feldman DE. 2006. Synaptic basis for whisker deprivation-induced synaptic depression in rat somatosensory cortex. J Neurosci. 26:4155–4165.

Carmignoto G, Vicini S. 1992. Activity-dependent decrease in NMDA receptor responses during development of the visual cortex. Science. 258:1007–1011.

Cheetham CE, Fox K. 2011. The role of sensory experience in presynaptic development is cortical area specific. J Physiol. 589:5691–5699.

Clements JD. 2003. Variance–mean analysis: a simple and reliable approach for investigating synaptic transmission and modulation. J Neurosci Methods. 130:115–125.

Cull-Candy S, Brickley S, Farrant M. 2001. NMDA receptor subunits: diversity, development and disease. Curr Opin Neurobiol. 11:327–335.

deKay JGT, Chang TC, Mills N, Speed HE, Dobrunz LE. 2006. Responses of excitatory hippocampal synapses to natural stimulus patterns reveal a decrease in short-term facilitation and increase in short-term depression during postnatal development. Hippocampus. 16:66–79.

Delaney AJ, Power JM, Sah P. 2012. Ifenprodil reduces excitatory synaptic transmission by blocking presynaptic P/Q type calcium channels. J Neurophysiol. 107:1571–1575.

Dobrunz LE, Stevens CF. 1997. Heterogeneity of release probability, facilitation, and depletion at central synapses. Neuron. 18:995–1008.

Dolev I, Fogel H, Milshtein H, Berdichevsky Y, Lipstein N, Brose N, Gazit N, Slutsky I. 2013. Spike bursts increase amyloid-beta 40/42 ratio by inducing a presenilin-1 conformational change. Nat Neurosci. 16:587–595.

Dumas TC. 2005. Late postnatal maturation of excitatory synaptic transmission permits adult-like expression of hippocampal-dependent behaviors. Hippocampus. 15:562–578.

Dumas TC, Foster TC. 1995. Developmental increase in CA3-CA1 presynaptic function in the hippocampal slice. J Neurophysiol. 73:1821–1828.

Durand GM, Konnerth A. 1996. Long-term potentiation as a mechanism of functional synapse induction in the developing hippocampus. J Physiol Paris. 90:313–315.

Feldman DE. 2009. Synaptic mechanisms for plasticity in neocortex. Annu Rev Neurosci. 32:33–55.

Fox K. 2002. Anatomical pathways and molecular mechanisms for plasticity in the barrel cortex. Neuroscience. 111: 799–814.

Freedman R, Adler LE, Myles-Worsley M, Nagamoto HT, Miller C, Kisley M, McRae K, Cawthra E, Waldo M, et al. 1996. Inhibitory gating of an evoked response to repeated auditory stimuli in schizophrenic and normal subjects: Human recordings, computer simulation, and an animal model. Arch Gen Psychiatry. 53:1114–1121.

Funahashi R, Maruyama T, Yoshimura Y, Komatsu Y. 2013. Silent synapses persist into adulthood in layer 2/3 pyramidal neurons of visual cortex in dark-reared mice. J Neurophysiol. 109:2064–2076.

Goel A, Jiang B, Xu LW, Song L, Kirkwood A, Lee H-K. 2006. Cross-modal regulation of synaptic AMPA receptors in primary sensory cortices by visual experience. Nat Neurosci. 9: 1001–1003.

Hanse E, Gustafsson B. 2001. Vesicle release probability and pre-primed pool at glutamatergic synapses in area CA1 of the rat neonatal hippocampus. J Physiol. 531:481–493.

Hanse E, Seth H, Riebe I. 2013. AMPA-silent synapses in brain development and pathology. Nat Rev Neurosci. 14:839–850.

Hengen KB, Lambo ME, Van Hooser SD, Katz DB, Turrigiano GG. 2013. Firing rate homeostasis in visual cortex of freely behaving rodents. Neuron. 80:335–342.

Hensch TK. 2005. Critical period plasticity in local cortical circuits. Nat Rev Neurosci. 6:877–888.

Hessler NA, Shirke AM, Malinow R. 1993. The probability of transmitter release at a mammalian central synapse. Nature. 366:569–572.

Hsia AY, Malenka RC, Nicoll RA. 1998. Development of excitatory circuitry in the hippocampus. J Neurophysiol. 79: 2013–2024.

Isaac JTR, Ashby MC, McBain CJ. 2007. The role of the GluR2 subunit in AMPA receptor function and synaptic plasticity. Neuron. 54:859–871.

Itskov PM, Vinnik E, Diamond ME. 2011. Hippocampal representation of touch-guided behavior in rats: persistent and independent traces of stimulus and reward location. PLoS One. 6:e16462.

Jitsuki S, Takemoto K, Kawasaki T, Tada H, Takahashi A, Becamel C, Sano A, Yuzaki M, Zukin RS, Ziff Edward B, et al. 2011. Serotonin mediates cross-modal reorganization of cortical circuits. Neuron. 69:780–792.

Kavalali ET. 2015. The mechanisms and functions of spontaneous neurotransmitter release. Nat Rev Neurosci. 16:5–16.

Keck T, Keller GB, Jacobsen RI, Eysel UT, Bonhoeffer T, Hubener M. 2013. Synaptic scaling and homeostatic plasticity in the mouse visual cortex in vivo. Neuron. 80:327–334.

Kirson ED, Yaari Y. 1996. Synaptic NMDA receptors in developing mouse hippocampal neurones: functional properties and sensitivity to ifenprodil. J Physiol. 497:437–455.

Kullmann DM. 1994. Amplitude fluctuations of dual-component EPSCs in hippocampal pyramidal cells: implications for long-term potentiation. Neuron. 12:1111–1120.

Kumaran D, Maguire EA. 2009. Novelty signals: a window into hippocampal information processing. Trends Cogn Sci. 13: 47–54.

Lambo ME, Turrigiano GG. 2013. Synaptic and intrinsic homeostatic mechanisms cooperate to increase L2/3 pyramidal neuron excitability during a late phase of critical period plasticity. J Neurosci. 33:8810–8819.

Lavenex P, Amaral DG. 2000. Hippocampal-neocortical interaction: a hierarchy of associativity. Hippocampus. 10:420–430.

Liao D, Malinow R. 1996. Deficiency in induction but not expression of LTP in hippocampal slices from young rats. Learn Mem. 3:138–149.

Lisman JE, Otmakhova NA. 2001. Storage, recall, and novelty detection of sequences by the hippocampus: elaborating on the SOCRATIC model to account for normal and aberrant effects of dopamine. Hippocampus. 11:551–568.

Maffei A, Nelson SB, Turrigiano GG. 2004. Selective reconfiguration of layer 4 visual cortical circuitry by visual deprivation. Nat Neurosci. 7:1353–1359.

Mierau SB, Meredith RM, Upton AL, Paulsen O. 2004. Dissociation of experience-dependent and -independent changes in excitatory synaptic transmission during development of barrel cortex. Proc Natl Acad Sci USA. 101: 15518–15523.

Monyer H, Seeburg PH, Wisden W. 1991. Glutamate-operated channels: developmentally early and mature forms arise by alternative splicing. Neuron. 6:799–810.

Pereira A, Ribeiro S, Wiest M, Moore LC, Pantoja J, Lin S-C, Nicolelis MAL. 2007. Processing of tactile information by the hippocampus. Proc Natl Acad Sci. 104:18286–18291.

Petersen CH, Crochet S. 2013. Synaptic computation and sensory processing in neocortical layer 2/3. Neuron. 78:28–48.

Philpot BD, Sekhar AK, Shouval HZ, Bear MF. 2001. Visual experience and deprivation bidirectionally modify the composition and function of NMDA receptors in visual cortex. Neuron. 29:157–169.

Plant K, Pelkey KA, Bortolotto ZA, Morita D, Terashima A, McBain CJ, Collingridge GL, Isaac JTR. 2006. Transient incorporation of native GluR2-lacking AMPA receptors during hippocampal long-term potentiation. Nat Neurosci. 9: 602–604.

Rosenmund C, Clements JD, Westbrook GL. 1993. Nonuniform probability of glutamate release at a hippocampal synapse. Science. 262:754–757.

Sans N, Petralia RS, Wang YX, Blahos J 2nd, Hell JW, Wenthold RJ. 2000. A developmental change in NMDA receptor-associated proteins at hippocampal synapses. J Neurosci. 20: 1260–1271.

Slutsky I, Abumaria N, Wu LJ, Huang C, Zhang L, Li B, Zhao X, Govindarajan A, Zhao MG, Zhuo M, et al. 2010. Enhancement of learning and memory by elevating brain magnesium. Neuron. 65:165–177.

Smith GB, Heynen AJ, Bear MF. 2009. Bidirectional synaptic mechanisms of ocular dominance plasticity in visual cortex. Philos Trans R Soc Lond B Biol Sci. 364:357–367.

Speed HE, Dobrunz LE. 2008. Developmental decrease in short-term facilitation at schaffer collateral synapses in hippocampus Is mGluR1 sensitive. J Neurophysiol. 99:799–813.

Squire LR, Stark CEL, Clark RE. 2004. The medial temporal lobe*. Annu Rev Neurosci. 27:279–306.

Stern EA, Maravall M, Svoboda K. 2001. Rapid development and plasticity of layer 2/3 maps in rat barrel cortex in vivo. Neuron. 31:305–315.

Tsodyks MV, Markram H. 1997. The neural code between neocortical pyramidal neurons depends on neurotransmitter release probability. Proc Natl Acad Sci USA. 94:719–723.

Vinogradova OS. 2001. Hippocampus as comparator: role of the two input and two output systems of the hippocampus in selection and registration of information. Hippocampus. 11: 578–598.

Wiesel TN, Hubel DH. 1963. Single-cell responses in striate cortex of kittens deprived of vision in one eye. J Neurophysiol. 26:1003–1017.

Witter MP, Groenewegen HJ, Lopes da Silva FH, Lohman AH. 1989. Functional organization of the extrinsic and intrinsic circuitry of the parahippocampal region. Prog Neurobiol. 33: 161–253.

Zheng J-J, Li S-J, Zhang X-D, Miao W-Y, Zhang D, Yao H, Yu X. 2014. Oxytocin mediates early experience-dependent cross-modal plasticity in the sensory cortices. Nat Neurosci. 17: 391–399.

Zucker RS, Regehr WG. 2002. Short-term synaptic plasticity. Annu Rev Physiol. 64:355–405.